Flow conditions in a side channel compressor

Dipl.-Ing. A. Krake, Univ. Prof. Dr.-Ing. K. Fiedler
University of the Federal Armed Forces
Laboratory for Turbomachinery
Holstenhofweg 85, 22043 Hamburg, Germany
Tel.: ++49 (0) 40 / 6541 - 2919
Fax: 2436
andreas.krake@unibw-hamburg.de

Abstract

The investigations concern the velocity distribution in the impeller and the side channel of a side channel compressor. Probe measurements were conducted to investigate the flow field in the side channel. For that a five-hole-pressure-probe and a thermocouple-probe were used to conventionally investigate the flow conditions in the side channel. The measurement positions were placed along the side channel. In addition to the probe studies laser-two-focus measurements were conducted. They enable to investigate the velocity field not only in the side channel but in the impeller sections too. The results of both, the probe measurements and the laser-two-focus studies complement each another. The first evaluated results give information about the flow characteristic. They confirm the streamline theory. With the new knowledge about the flow field the Laboratory for Turbomachinery intends to improve calculation models and suggest an opportunity to improve side channel machines.

Nomenclature

A_{sc}	[m²]	cross section of the side channel	$\dot{V}_s$	[m³/s]	volume flow
c_p	[J/kg K]	thermal capacity	T_t	[K]	total temperature
Δh_s	[J/kg]	isentropic enthalpie rise	T_{td}	[K]	total outlet temperature
p_s	[bar]	intake pressure	T_u	[%]	Turbulence
p_d	[bar]	outlet pressure	u_m	[m/s]	mean circumferential velocity
P_{el}	[W]	electric power	j	[-]	flow number
s	[m]	distance of focal points	y	[-]	pressure number
t	[s]	time of flight	h	[-]	efficiency
T_s	[K]	intake temperature	h_m	[-]	efficiency of the motor

Introduction

Side channel machines are a special kind of turbo machines. Commonly used as pumps or compressors they enable the compression of fluids in a multi stage process depending on the operating conditions.

Figure 1 shows the principal design of a side channel maschine. It consist of an impeller and a side channel. The shape of the side channel looks like the large Greek symbol Omega. The impeller is equipped with blades that form impeller sections and rotates opposite to the side channel. Both, the side channel and the impeller, commonly have a semi-circle cross section. Thus the fluid follows the flow

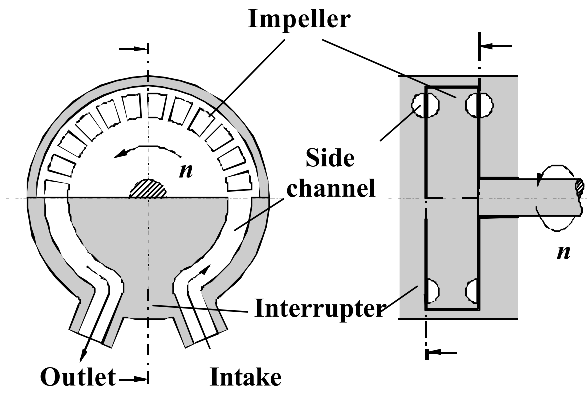

Fig. 1: Scheme **of a side channel compressor**

channel in the rotating direction of the impeller. The intake is seperated from the outlet by an interrupter. The design type of the double-flow machine being investigated at the Laboratory for Turbomachinery is shown in figure 2.

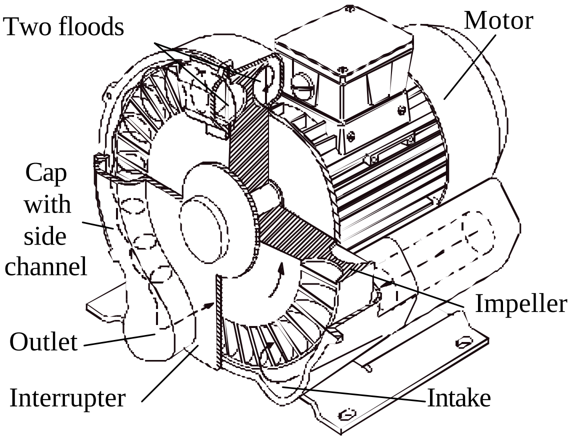

Fig. 2: Double entry side channel compressor

Based on previous experimental studies [e.g. Engels, 1940; Gabi, 1982; Hübel, 1996] the streamline theory was developed. This description model bases on the fact, that the fluid in the side channel rotates with a lower circumferential speed than in the impeller sections. It is assumed, that the higher centrifugal forces within the fluid in the impeller section cause a spiral flow through the impeller and the side channel. The spiral flow is shown in figure 2.

Previous conventional probe measurements on side channel pumps could only be conducted in the side channel. Other investigations observing colour injections made it necessary to modify the original shape of the flow channel. With the laser-two-focus anemometry the Laboratory for Turbomachinery carries out measurements avoiding these problems. For the first time it is realised to measure the three-dimensional velocity field of the compressible fluid in the hole compressor flow channel.

Performance map

The investigated industrial compressor is a commonly used double entry side channel machine with a mean diameter of 358 mm. The two impellers are built back to back to minimize the axial force. The flow field investigations are concerning the impeller and the side channel facing to the front of the compressor.

To ensure that the different studies can be compared, the operating characteristic of the machinery was determined by measuring the performance map.

External measurements at the intake and the outlet of the compressor cannot specify the inner flow conditions in the investigated flood. That is why the mass flow through both floods is constructively caused not equal. To exclude the influence of the not investigated flood, that impeller was exchanged by a flat disk. Additionally the flanges to the passivated side channel were closed. With this modified construction all investigations were conducted.

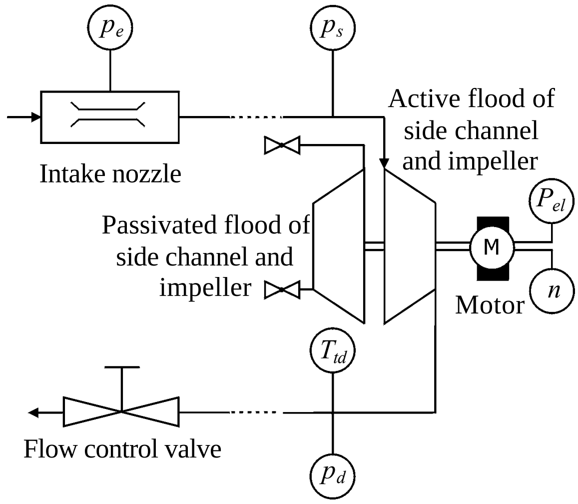

Fig. 3: Diagram of experimental arrangement

Figure 3 shows the flow diagram of the installation used to measure the operating points and points out the measuring positions. The compressor sucks the ambient air through a ISA-1932-nozzle [DIN EN ISO, 1995]. The intake velocity varies between 11 m/s and 42 m/s. This is equivalent to a mass flow of 0,027 kg/s up to 0,096 kg/s. The mass flow is calculated with the ambient temperature, the ambient pressure and the pressure loss of the nozzle. An approximately 3 m long flexible tube connects the intake with the machine flange.

At the intake of the machine a second static pressure measurement takes place. It is used to calculate the input volume flow to the compressor. Inside the machine the air is compressed. Two kinds of impellers are in use. One has simple radial blades. The other is equipped with vanes that are inclined forwards. After passing the machine the total temperature and the static pressure of the air is measured.

The heated air (up to 105 °C) is lead to the flow control valve by an 3 m long tube. After passing the valve the air is blown into the atmosphere.

To characterise the operation point common non-dimensional numbers are used. The flow number *j* is calculated for describing the flow through the machine:

$$j = \dot{V}_s \big/ (u_m \cdot A_{sc}) \ . \qquad (1)$$

It is a function of the volume flow $\dot{V}_s$ through the machine flange, the mean circumferential velocity u_m, and the cross section of the side channel A_{sc}.
The pressure number y gives information about the energy transfer to the fluid in the compressor. It can be defined as the quotient of the fluid isentropic enthalpy rise Δh_s and the square power of the mean circumferential velocity u_m

$$y = \frac{\Delta h_s}{u_m^2/2} \; . \tag{2}$$

The isentropic enthalpy rise is calculated with the thermal capacity c_p, the static intake temperature T_s and the static pressures at the machine flanges by:

$$\Delta h_s = c_p \cdot T_s \cdot \left[\left(\frac{p_d}{p_s} \right)^{\frac{k-1}{k}} - 1 \right] . \tag{3}$$

The efficiency h is defined as the quotient of the product of isentropic enthalpie rise Δh_s and mass flow $\dot{m}$ and the input power:

$$h = \frac{\dot{m} \cdot \Delta h_s}{P_{el} \cdot h_m} \; . \tag{4}$$

Because of the considerable heat losses a thermally defined efficiency is not used.

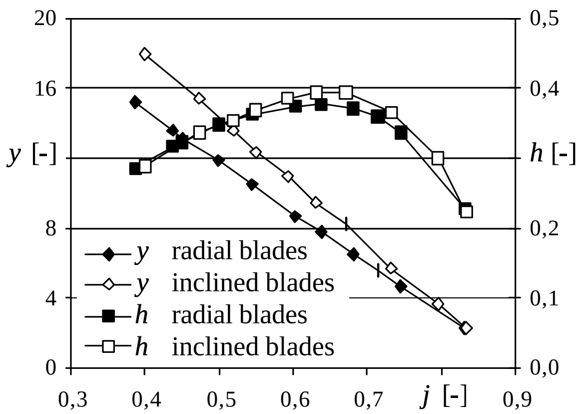

Fig. 4: Performance map

The conducted measurements on the modified compressor lead to an performance map that is shown in figure 4.
Characteristic for side channel compressors is the steep rise of the pressure number by a decreasing flow number. The reason is, that the axial pitch of the spiral flow decrease with a higher pressure difference from the intake to the outlet. By this the fluid more often passes the impeller and the impulse transfer increases. That is why side channel machines do not have a surge limit.

The efficiency maximum of both impellers appear at the flow number $j \approx 0{,}65$. In the area of higher pressure numbers the inner leakage losses increase and the efficiencys decrease. If the flow number rises the spiral curve is widened and the flow velocity increases. Friction losses at intake and outlet increase. That is why in the region of higher flow numbers the efficiency drops down.
Comparing the performance maps of both impeller variants it is evident, that the constellation with forwards inclined blades produces higher pressure ratios at higher efficiency. This agrees with previous studies. The spiral flow is better controlled by inclined blades. This can be proven by observing the velocity triangles [Bender, 1984].
For the probe measurements and the laser-2-focus measurements the maximum efficient operation point $j = 0{,}65$ was chosen. Additional measurements were conducted at the operating limits $j = 0{,}42$ and $j = 0{,}75$. The following details deal with the operating point $j = 0{,}65$. With further evaluations the Laboratory of Turbomachinery will compare the current results with the data of the limit operating points.

Probe measurements

The probe measurements in the side cannel were the first step to verify the flow conditions in the investigated compressor. They were conducted with the calibrated five-hole-pressure-probe shown in figure 5. Using multiparameter approximation the Mach number, the total and the static pressures can be calculated from the five pressure values.

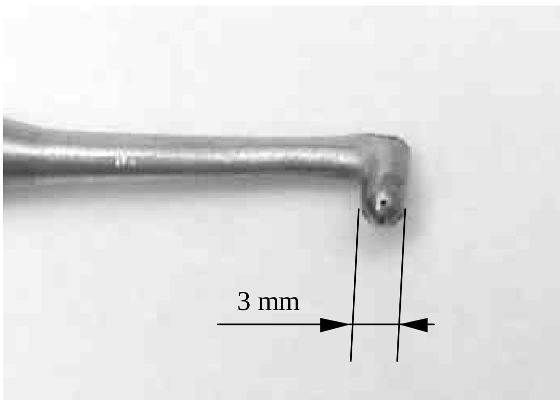

Fig. 5: Fife-hole-pressure-probe

To calculate the flow velocity by the perfect gas equation and Bernoulli's equation it is necessary to know the flow temperature at the measuring point. Therefore a temperature probe consisting of a thermocouple was used. To realise the measurements the temperature probe and the pressure probe were led through an inset into the side channel. The temperature probe and the inset are shown in figure 6.

Fig. 6: Temperature probe at the inset

The inset can be mounted in the cap at different positions. The drawings in figure 7 show the view to the front of the cap and the used insets. The various insets allow to put the probes into the side channel in different angles to the axial plane.

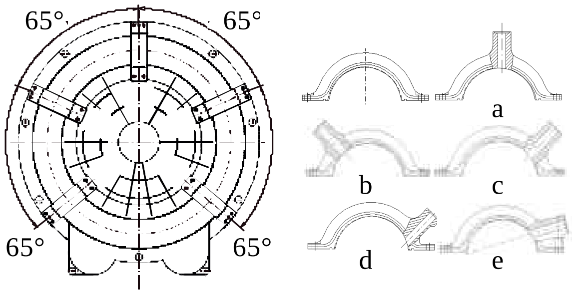

Fig. 7: Design of the modified cap and the insets

The presented results are received at the 12 o'clock position. At first the pressure measurements were made. For measuring the pressure values the probe was turned around its shaft into the flow direction. Then the measurement was started and the angle position was taken. After the pressure measurements the temperature probe was put into the inset. While measuring the temperature the thermocouple head was moved, exactly the same way as the pressure probe. Thus the temperature values almost correspond approximately to the total temperature of the fluid. This way it would be possible to calculate the velocity distribution in the observed cross section.

As an example the temperature profile measured while using radial blades and the inset a) is shown in figure 8. The detected temperature profile along the positions of the thermo head always lies within the limits of two Kelvin. Because the temperature effect on the velocity determination is small, the flow field was calculated with the temperature at the half way position.

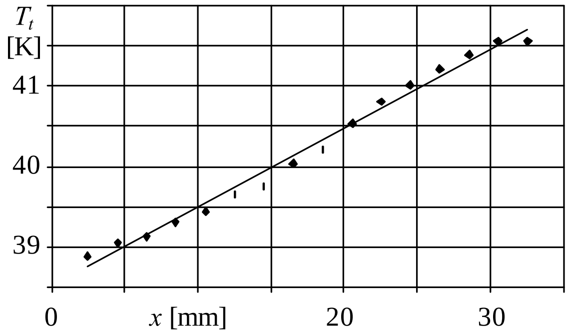

Fig. 8: Temperature distribution

The calculated flow fields of the side channel are shown in figure 9 to 12. The mean flow direction corresponds with the *z* axis. The impeller has a local rotating velocity u. The contour is equivalent to the shape of the side channel. The probe measurements were conducted along the drawn lines. The velocity values and directions are shown by the vector arrows.

Unfortunately lots of the probe measurements could not be used because the probe could not be adjusted in the current flow direction by turning it around its shaft. Thus the flow data is outside the calibration limits of the pressure probe. But the received results give a first impression of the common flow character inside the flow channel.

Figure 9 shows the absolute velocity in the side channel by using the impeller with radial blades. The drawn vectors clearly show the spiral flow. In the inner section the relative flow directions to the probe do not allow to calculate correct velocity values.

Figure 10 shows the velocity field at the same operating point by using the impeller with inclined blades. The typical spiral flow character is evident. But the swirl centre seems to be moved in direction *x* to the inlet of the side channel. At the outlet area of the side channel the flow direction strongly differs from the possible probe positions. There was only one opportunity to measure the velocity vector near the side channel wall.

Figures 11 and 12 show the relative velocity values in the measured area. For this the local circumferential velocity of the impeller *u* was subtracted from the flow velocity component in *z*-direction. The results support the assumption of the moving vortex centre.

In figure 11 the marked vortex centre lies near the *y*-axis. The common relative flow direction moves around this centre. Thereby the fluid leaves the impeller sections and enters the side channel with a circumferential speed that corresponds to the rotating velocity of the impeller. On its way to the side channel outlet the fluid is decelerated, so that the circumferential speed of the entrance to the

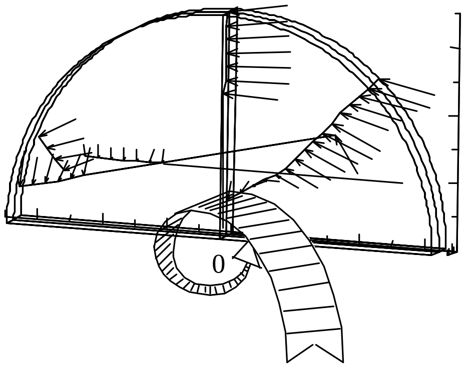

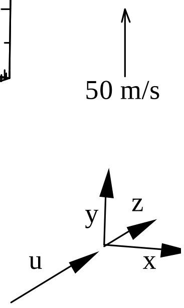

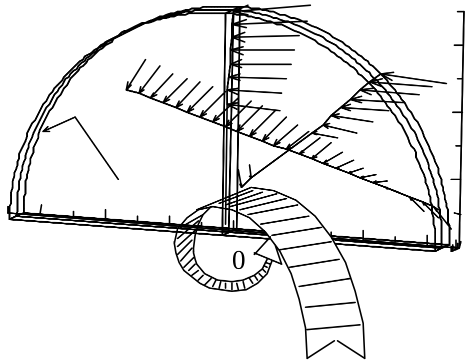

Fig. 9: Absolute side channel flow (impeller with radial blades)

Fig. 10: Absolute side channel flow (impeller with inclined blades)

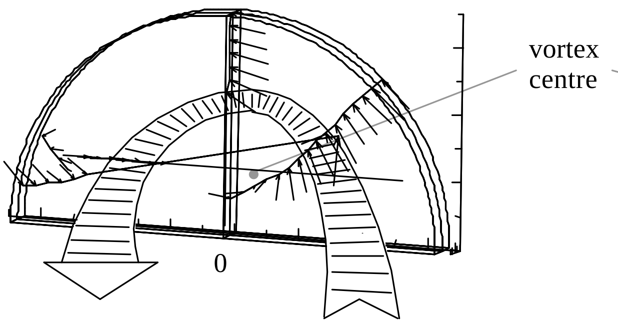

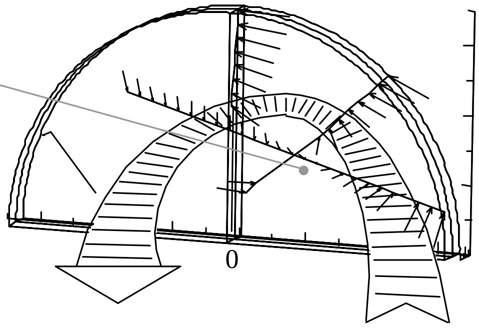

Fig. 11: Relative side channel flow (impeller with radial blades)

Fig. 12: Relative side channel flow (impeller with inclined blades)

impeller area is lower than the local impeller rotating velocity.
The same fact is shown in figure 12 with the impeller consisting of inclined blades. Because of the inclined blades the circumferential speed of the fluid at the side channel entrance is higher than the local impeller velocity. It is assumed that the fluid will be decelerated at the side channel outlet too.
Unfortunately the lack of correct probe measurements does not allow a clear presentation of the local velocity values at the impeller entrance. But the moved rotation centre can clearly be seen. It is nearly positioned in the middle of the side channel entrance sector.
While measuring with the temperature and the pressure probe generally the error influences have to be observed. The first point is the effect of the probe on the measured stream characteristic. But at the presented operating point it is, because of the spiral flow, improbable that the wake of the probe head directly influences the measurement. However to fix the operating point it was necessary to adjust the control valve newly after setting in the probe.
The second problem to be mentioned is the thickness of the probe heads. They have the size of circa 10 % of the side channel radius. This causes a distortion of the evaluated velocity especially if the velocity gradient on the way of the probes through the flow area is high. The reason is the difference of the static and total pressure values along the probe way. This can not only cause incorrect velocity values but also flow angles that are differing from the current flow direction. This might be the reason why the received velocity vectors presented in fig. 9 to 12 differ from each other near the intersecting points of two probe ways.
A principal measuring problem appeared when it was tried to measure the flow field near the compressor inlet at the 4 o'clock and the 2 o'clock position. The turbulence caused by the entering air stream made it impossible to adjust the probe in a defined flow direction. Additionally it is suggested, that the interrupter stops the circulation of the fluid around the mentioned rotation centre. The impeller sections transport the decelerated compressed air along the interrupter, so that the fluid expands in the direction of the low pressure inlet area. The high turbulence did not allow any useful probe measurement until the spiral flow is re-established.

Laser-2-Focus-Measurement

Because of the above mentioned difficulties in connection with probe measurements, the Laboratory of Turbomachinery investigates the flow field by applying the non-intrusive laser-2-focus-anemometry (L2F), which does not cause any disturbance of the flow. The principal L2F measurement scheme is shown in figure 13.

The argon laser equipment produces two focal points in the measuring volume. The measured part of the air stream flows through this area. The flow has to be seeded with tracer particles with diameter no bigger than 0,4 µm. If these particle pass the two focal points the detected scattered light produces two electronic impulses. The first one starts a time measurement. The second impulse stops it. The velocity can be calculated with the known distance s of the two focal points.

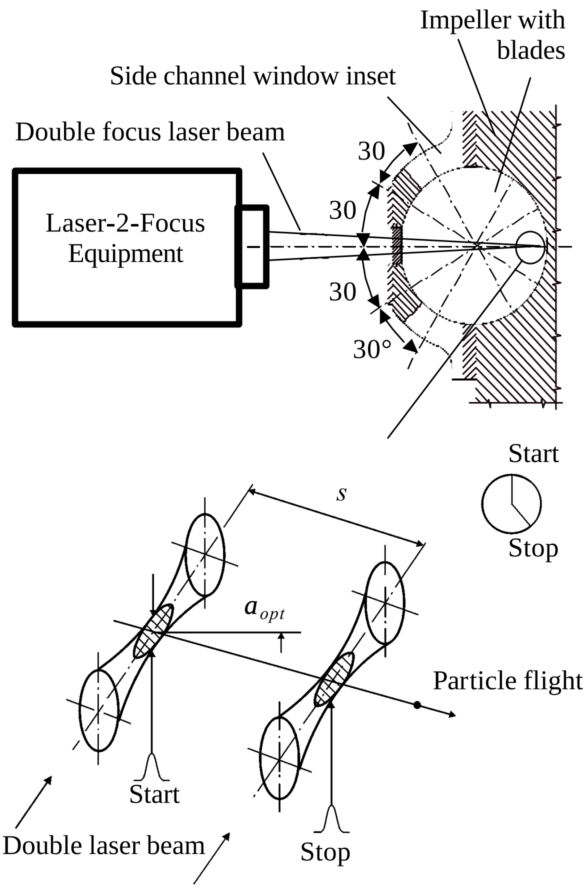

Fig. 13: Principal measurement scheme

During the measurement the stop focal point is stepwise turned around the start focus. Thus in each angular position of the optical head a histogram of transit times and flow angles is received. To receive the mean value and direction of the velocity the data is evaluated with statistical methods. The results give information about the velocity vector of the measurement plane. An detailed description of the measuring system and the calculating procedures can be found by [Schodl, 1977].

To investigate the flow channel five window insets symbolised in figure 13 were used. Their optical axis differ by an angle of 30° . The insets can be mounted at the positions shown in figure 7. This way it is theoretically possible to reach each point inside the flow channel with the laser focal volume. Since the measurement mainly takes place inside the rotating blade channels the L2F system has to be synchronised with the rotating impeller. The strongly scattered light of the blade surfaces, passing through the laser beam, could destroy the laser equipment. Therefore the laser beam is optically switched off while the blades pass the measuring volume. The measuring interval inside a blade channel is divided into a number of windows. The measured points within these windows move through the laser focal volume. The positions of the measuring points within the blade channels correspond to the specific measuring windows of the laser system.

As shown in figure 14 the passing time of one blade channel and the both bordering blades is divided into 32 windows. During the blade reflection period the laser beam is switched off. During this blind period the laser system can not detect the flow data. Inside the blade channels the L2F system works and the velocity data of the several windows is registered. This procedure is repeating each time when the next blade channel passes. The

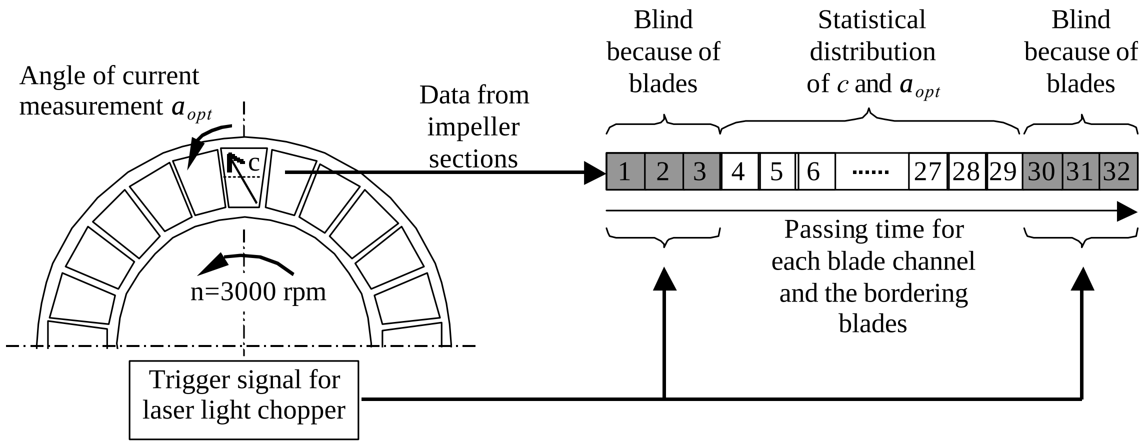

Fig. 14: Diagram of triggering the measurement periods and the light chopper

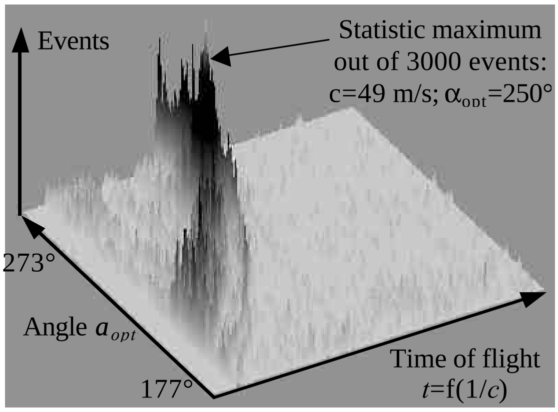

Fig. 15: Statistic event distribution

measurement process is ended when a defined number of measurement events is reached.

All registered data of each measuring interval is statistically evaluated. A distribution example of all data of one window is shown in figure 15.

The synchronisation is realised by a reflex light barrier. It is placed at the 6 o'clock position in the middle of the interrupter. To optimise the reflection the blade edges were painted white. The other surfaces of the blade channel are painted black to prevent measuring errors by scattered light.

The tracer particles are generated in an aerosol generator. They are injected into the flow channel at the 4 o'clock position. The used lance injects the particles into the turbulent intake area as shown in figure 16.

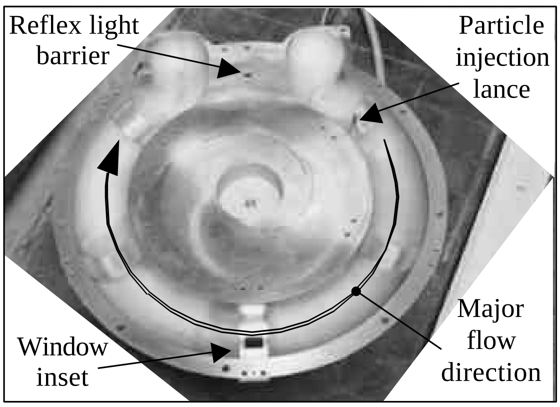

Fig. 16: The prepared side channel cap

The relative translation between the compressor and the laser equipment is realised by the traverse system of the optical head. A special construction was designed which gives the opportunity to rotate the compressor around two axes. The experimental set-up is shown in figure 17.

The first investigations were made with the impeller equipped with radial blades at the 12 o'clock position. In this case it is not necessary to turn the compressor around its vertical axis. The used

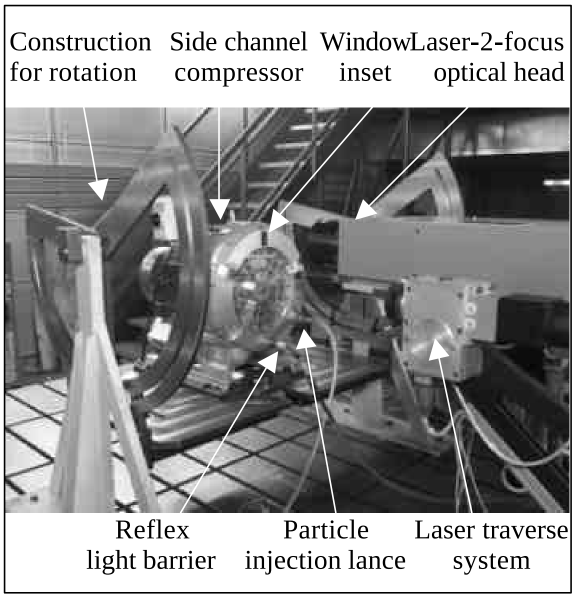

Fig. 17: Experimental set-up

window inset is drawn in figure 13. This way it is possible to receive 2-dimensional flow data of the plane vertical to the laser beam.

The measurements were mainly conducted in the middle of the blade channel opposite the window inset. Because the rotation centre of the flow lies in front of the blade edges the measurements were expended to the side channel area. Under consideration of a readable presentation only random fife percent of the received velocity data of the measurement area are shown in figure 18. When evaluating the positions of the velocity data the refraction of the window insets was considered. The drawn contour explains the blade channel shape.

The shown 2-dimensional velocity vectors clearly show the spiral flow character. The velocity values correspond to the results of the probe measurements. The fact that the general velocity direction in the observed side channel area corresponds to the blade channel flow supports the assumption that the rotation centre of the spiral flow is located inside the side channel. Both these results lead to the

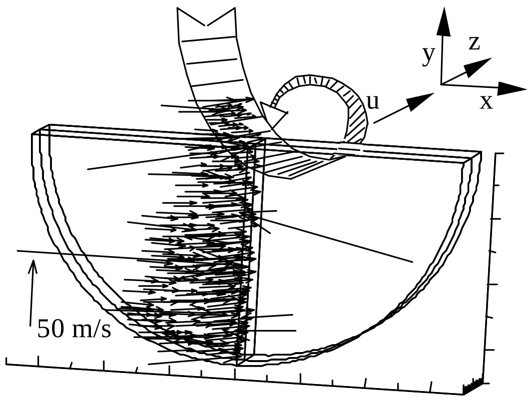

Fig. 18: Absolute blade channel flow

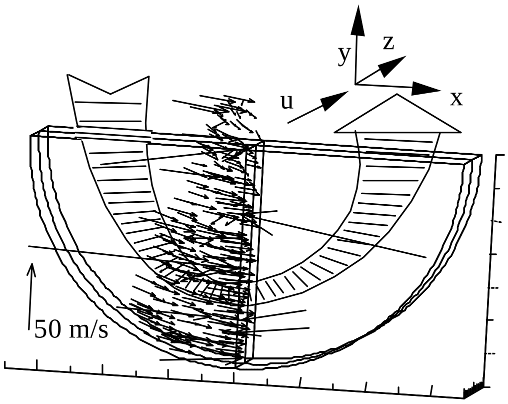

Fig. 19: Relative blade channel flow

assumption that the actual velocity direction nearly corresponded with the measurement planes.
Figure 19 shows the relative flow field data. At the impeller intake area the acceleration of the fluid is evident. In the first third of its way through the blade channels the fluid is accelerated up to the circumferential speed of the impeller. On its way along the inner impeller section the flow mainly follows the blade channel contour.
But the presented results in figure 18 and 19 show some vector arrows that do not correspond to the common velocity values and directions. The arrow heads are positioned at the measuring points. It can clearly be seen that the error date concentrates in the areas near the wall and in the side channel region. The reason is the detected flow field turbulence. The calculated turbulence data is shown in the cross section of figure 20.
The first turbulence concentration area is located near the impeller walls. The reason might be the boundary layer. But checking the dimensions of the casted impeller differences of the blade pitch of more than fife percent were detected. Thus it is assumed that some of the evaluated near wall measurement points lie inside the impeller blades. In future they can be filtered by testing the local values of turbulence and velocity.
The second turbulence area lies in the side channel region. Near the assumed rotation centre the turbulence rises strongly. Following the L2F instructions flow measurements with turbulence values over 20% have to be rejected. Therefore the measurement were stopped before reaching the rotation centre.

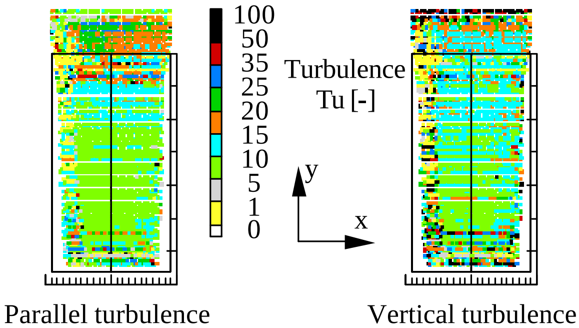

Fig. 20: Turbulence distribution

Conclusion and outlook

The conducted probe and laser-2-focus measurements inside the side channel and the impeller of a side channel compressor support the theory of a spiral fluid transport.
The Laboratory of Turbomachinery is conducting laser-2-focus measurements at additional possible side channel and impeller positions. By taking measurements at the same flow field point under various angular positions of the laser axis it is intended to evaluate 3-dimensional flow field data with an improved evaluation program.
Having identified the brake down of the vortex at the interrupter the Laboratory of Turbomachinery designed a modified cap to stabilize the spiral rotation of the fluid. This bladed interrupter shown in figure 21 will be tested soon.

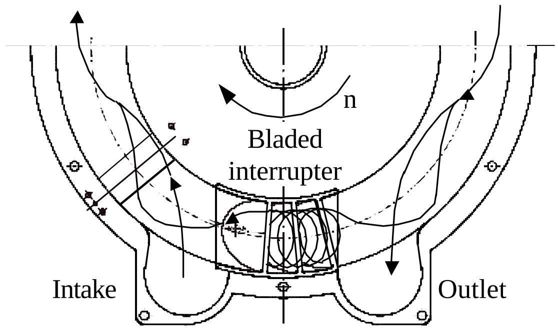

Fig. 21: Cap with bladed interrupter

References

Bender, A.: Untersuchungen an Seitenkanalverdichtern im Hinblick auf den Einsatz als Spülgebläse, Dissertation, RWTH Aachen, 1984

Engels, H.: Untersuchungen an Ringpumpen, Dissertation, TH Hannover, 1940

Gabi, M.: Theoretische und experimentelle Untersuchung der Strömung in Seitenkanalverdichtern, Dissertation, Universität. Karlsruhe, 1982

Hübel, M.: Experimentelle und theoretische Untersuchung der Innenströmung in einer Seitenkanalpumpe zur Kraftstofförderung in Einspritzsystemen von Ottomotoren, Dissertation, Universität Karlsruhe, 1996

Schodl, R.: Entwicklung des Laser-Zwei-Fokus-Verfahrens für die berührungslose Messung der Strömungsvektoren insbesondere in Turbomaschinen, Dissertation, RWTH Aachen, 1977